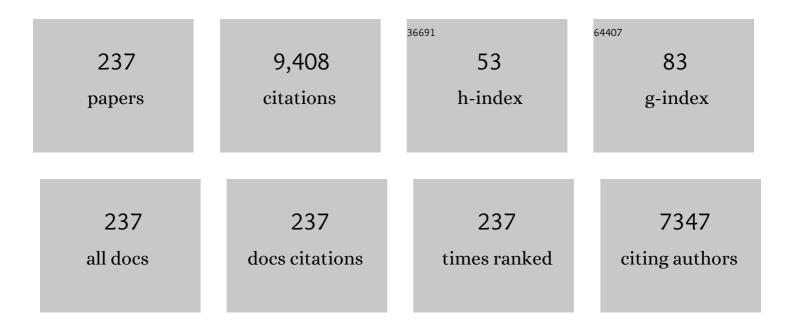
S Van Der Zwaag

List of Publications by Year in descending order

Source: https://exaly.com/author-pdf/10428011/publications.pdf Version: 2024-02-01



S VAN DED ZWAAC

#	Article	IF	CITATIONS
1	Local strain-induced energy storage as driving force for autogenous scratch closure. Journal of Materials Chemistry A, 2022, 10, 7073-7081.	5.2	4
2	Modelling the growth and filling of creep-induced grain-boundary cavities in self-healing alloys. Journal of Materials Science, 2022, 57, 12034-12054.	1.7	1
3	Surface precipitation of supersaturated solutes in a ternary Fe–Au–W alloy and its binary counterparts. Journal of Materials Science, 2021, 56, 5173-5189.	1.7	6
4	Contributions to Dynamic Behaviour of Materials Professor John Edwin Field, FRS 1936–2020. Journal of Dynamic Behavior of Materials, 2021, 7, 353-382.	1.1	1
5	A novel 3D mixed-mode multigrain model with efficient implementation of solute drag applied to austenite-ferrite phase transformations in Fe-C-Mn alloys. Acta Materialia, 2021, 212, 116897.	3.8	15
6	Precipitation of supersaturated solute in H ion irradiated Fe-Au and Fe-Au-W alloys studied by positron annihilation spectroscopy. Nuclear Instruments & Methods in Physics Research B, 2021, 505, 50-57.	0.6	4
7	Effect of topological imperfections on the electroâ€mechanical properties of structured piezoelectric particulate composites. JPhys Materials, 2020, 3, 014004.	1.8	1
8	Detailed In Situ Hot Stage Transmission Electron Microscope Observations of the Localized Pinning of a Mobile Ferrite-Austenite Interface in a Fe-C-Mn Alloy by a Single Oxidic Particle. Metallurgical and Materials Transactions A: Physical Metallurgy and Materials Science, 2020, 51, 3811-3818.	1.1	2
9	Competitive Healing of Creep-Induced Damage in a Ternary Fe-3Au-4W Alloy. Metallurgical and Materials Transactions A: Physical Metallurgy and Materials Science, 2020, 51, 4442-4455.	1.1	12
10	Direct TEM observation of α/γ interface migration during cyclic partial phase transformations at intercritical temperatures in an Fe-0.1CÂâ°'0.5Mn alloy. Acta Materialia, 2019, 178, 68-78.	3.8	7
11	Kinetics of zircon formation in yttria partially stabilized zirconia as a result of oxidation of embedded molybdenum disilicide. Acta Materialia, 2019, 174, 206-216.	3.8	9
12	Flexible, printed, Pb-free piezo-composites for haptic feedback systems. , 2019, , .		1
13	BiFeO ₃ synthesis by conventional solid-state reaction. , 2019, , .		6
14	Self healing of creep damage in iron-based alloys by supersaturated tungsten. Acta Materialia, 2019, 166, 531-542.	3.8	22
15	Selfâ€healing glass fiber reinforced polymer composites based on montmorillonite reinforced compartmented alginate fibers. Polymer Composites, 2019, 40, 471-480.	2.3	2
16	Synergetic active corrosion protection of AA2024-T3 by 2D- anionic and 3D-cationic nanocontainers loaded with Ce and mercaptobenzothiazole. Corrosion Science, 2018, 135, 35-45.	3.0	55
17	Protecting the MoSi2 healing particles for thermal barrier coatings using a sol-gel produced Al2O3 coating. Journal of the European Ceramic Society, 2018, 38, 2728-2734.	2.8	32
18	The effect of the TiC particle size on the preferred oxidation temperature for self-healing of oxide ceramic matrix materials. Journal of Materials Science, 2018, 53, 5973-5986.	1.7	35

#	Article	IF	CITATIONS
19	A Novel Approach for Controlling the Band Formation in Medium Mn Steels. Metallurgical and Materials Transactions A: Physical Metallurgy and Materials Science, 2018, 49, 1998-2010.	1.1	6
20	Analysis of the Grain Size Evolution for Ferrite Formation in Fe-C-Mn Steels Using a 3D Model Under a Mixed-Mode Interface Condition. Metallurgical and Materials Transactions A: Physical Metallurgy and Materials Science, 2018, 49, 41-53.	1.1	11
21	In Situ 3D Neutron Depolarization Study of the Transformation Kinetics and Grain Size Evolution During Cyclic Partial Austenite-Ferrite Phase Transformations in Fe-C-Mn Steels. Metallurgical and Materials Transactions A: Physical Metallurgy and Materials Science, 2018, 49, 5962-5975.	1.1	3
22	Modelling study on the three-dimensional neutron depolarisation response of the evolving ferrite particle size distribution during the austenite–ferrite phase transformation in steels. Philosophical Magazine, 2018, 98, 1884-1899.	0.7	1
23	Reply to Comment on "Monitoring Network and Interfacial Healing Processes by Broadband Dielectric Spectroscopy: A Case Study on Natural Rubber― ACS Applied Materials & Interfaces, 2017, 9, 14552-14554.	4.0	6
24	In-situ poling and structurization of piezoelectric particulate composites. Journal of Intelligent Material Systems and Structures, 2017, 28, 2467-2472.	1.4	18
25	Linking Surface Precipitation in Fe-Au Alloys to Its Self-healing Potential During Creep Loading. Metallurgical and Materials Transactions A: Physical Metallurgy and Materials Science, 2017, 48, 2109-2114.	1.1	12
26	Non-destructive monitoring of delamination healing of a CFRP composite with a thermoplastic ionomer interlayer. Composites Part A: Applied Science and Manufacturing, 2017, 101, 243-253.	3.8	35
27	Highly sensitive piezo particulate-polymer foam composites for robotic skin application. Ferroelectrics, 2017, 515, 25-33.	0.3	13
28	Effect of the polymer structure on the viscoelastic and interfacial healing behaviour of poly(urea-urethane) networks containing aromatic disulphides. European Polymer Journal, 2017, 97, 120-128.	2.6	44
29	Healing of a glass fibre reinforced composite with a disulphide containing organic-inorganic epoxy matrix. Composites Science and Technology, 2017, 152, 85-93.	3.8	39
30	Functionally graded ferroelectric polyetherimide composites for high temperature sensing. Journal of Materials Chemistry C, 2017, 5, 9389-9397.	2.7	18
31	Large area and flexible micro-porous piezoelectric materials for soft robotic skin. Sensors and Actuators A: Physical, 2017, 263, 554-562.	2.0	28
32	Crack healing behaviour of Cr 2 AlC MAX phase studied by X-ray tomography. Journal of the European Ceramic Society, 2017, 37, 441-450.	2.8	41
33	Poling piezoelectric (K,Na,Li)NbO ₃ -polydimethylsiloxane composites. Ferroelectrics, 2017, 515, 68-74.	0.3	9
34	Structure, dielectric and piezoelectric properties of donor doped PZT ceramics across the phase diagram. Ferroelectrics, 2016, 504, 160-171.	0.3	48
35	A combined fracture mechanical – rheological study to separate the contributions of hydrogen bonds and disulphide linkages to the healing of poly(urea-urethane) networks. Polymer, 2016, 96, 26-34.	1.8	77
36	Monitoring Network and Interfacial Healing Processes by Broadband Dielectric Spectroscopy: A Case Study on Natural Rubber. ACS Applied Materials & Interfaces, 2016, 8, 10647-10656.	4.0	51

#	Article	IF	CITATIONS
37	Self-Healing Corrosion-Protective Sol–Gel Coatings Based on Extrinsic and Intrinsic Healing Approaches. Advances in Polymer Science, 2016, , 185-218.	0.4	14
38	Effect of curing on the mechanical and healing behaviour of a hybrid dual network: a time resolved evaluation. RSC Advances, 2016, 6, 91806-91814.	1.7	17
39	Autonomous Filling of Grain-Boundary Cavities during Creep Loading in Fe-Mo Alloys. Metallurgical and Materials Transactions A: Physical Metallurgy and Materials Science, 2016, 47, 4831-4844.	1.1	25
40	Demonstrating the self-healing behaviour of some selected ceramics under combustion chamber conditions. Smart Materials and Structures, 2016, 25, 084019.	1.8	32
41	Autonomous filling of creep cavities in Fe-Au alloys studied by synchrotron X-ray nano-tomography. Acta Materialia, 2016, 121, 352-364.	3.8	33
42	Effect of the Dianhydride/Branched Diamine Ratio on the Architecture and Room Temperature Healing Behavior of Polyetherimides. ACS Applied Materials & Interfaces, 2016, 8, 34068-34079.	4.0	90
43	Computational modeling of structure formation during dielectrophoresis in particulate composites. Computational Materials Science, 2016, 112, 139-146.	1.4	15
44	Autonomous Repair Mechanism of Creep Damage in Fe-Au and Fe-Au-B-N Alloys. Metallurgical and Materials Transactions A: Physical Metallurgy and Materials Science, 2015, 46, 5656-5670.	1.1	24
45	A temperature oscillation instrument to determine pyroelectric properties of materials at low frequencies: Towards elimination of lock-in methods. Review of Scientific Instruments, 2015, 86, 105111.	0.6	3
46	Piezoelectric Lead Zirconium Titanate Composite Touch Sensors for Integration with Flexible OLED Technology. Ferroelectrics, 2015, 480, 1-9.	0.3	4
47	Direct and indirect observation of multiple local healing events in successively loaded fibre reinforced polymer model composites using healing agent-filled compartmented fibres. Composites Science and Technology, 2015, 106, 127-133.	3.8	31
48	Overview of the current issues in austenite to ferrite transformation and the role of migrating interfaces therein for low alloyed steels. Materials Science and Engineering Reports, 2015, 92, 1-38.	14.8	136
49	Microstructural and X-ray tomographic analysis of damage in extruded aluminium weld seams. Materials Science and Technology, 2015, 31, 94-104.	0.8	10
50	On the use of B-alloyed MoSi 2 particles as crack healing agents in yttria stabilized zirconia thermal barrier coatings. Journal of the European Ceramic Society, 2015, 35, 4507-4511.	2.8	64
51	Analysis of the mobility of migrating austenite–ferrite interfaces. Philosophical Magazine, 2015, 95, 2899-2917.	0.7	19
52	Correlation between scratch healing and rheological behavior for terpyridine complex based metallopolymers. Journal of Materials Chemistry A, 2015, 3, 22145-22153.	5.2	79
53	Piezoelectric and pyroelectric properties of conductive polyethylene oxide-lead titanate composites. Smart Materials and Structures, 2015, 24, 045020.	1.8	17
54	On the interfacial healing of a supramolecular elastomer. Polymer, 2015, 56, 435-442.	1.8	41

#	Article	IF	CITATIONS
55	A Comparative Study of the Microstructure and Mechanical Properties of α + β Titanium Alloys. Metal Science and Heat Treatment, 2014, 56, 374-380.	0.2	5
56	Effect of Heat Treatment on Microstructure and Properties with Compression of Metastable Î ² -Titanium Alloy. Metal Science and Heat Treatment, 2014, 56, 245-252.	0.2	1
57	Piezoelectric and pyroelectric properties of lead titanate-polyethylene oxide composites. , 2014, , .		2
58	Effect of dielectrophoretic structuring on piezoelectric and pyroelectric properties of lead titanate-epoxy composites. Smart Materials and Structures, 2014, 23, 105030.	1.8	40
59	A strain-based computational design of creep-resistant steels. Acta Materialia, 2014, 64, 133-143.	3.8	19
60	Positron annihilation study on deformation-induced Au precipitation in Fe–Au and Fe–Au–B–N alloys. Journal of Materials Science, 2014, 49, 2509-2518.	1.7	12
61	Preferential Au precipitation at deformation-induced defects in Fe–Au and Fe–Au–B–N alloys. Journal of Alloys and Compounds, 2014, 584, 425-429.	2.8	16
62	Piezoelectric and mechanical properties of fatigue resistant, self-healing PZT–ionomer composites. Smart Materials and Structures, 2014, 23, 055001.	1.8	36
63	Review of current strategies to induce self-healing behaviour in fibre reinforced polymer based composites. Materials Science and Technology, 2014, 30, 1633-1641.	0.8	53
64	Mechanical stability of individual austenite grains in TRIP steel studied by synchrotron X-ray diffraction during tensile loading. Materials Science & Engineering A: Structural Materials: Properties, Microstructure and Processing, 2014, 618, 280-287.	2.6	48
65	Effect of Free Surface on the Stability of Individual Retained Austenite Grains in a Duplex Stainless Steel. Metallurgical and Materials Transactions A: Physical Metallurgy and Materials Science, 2014, 45, 4875-4881.	1.1	16
66	The mechanical stability of retained austenite in low-alloyed TRIP steel under shear loading. Materials Science & Engineering A: Structural Materials: Properties, Microstructure and Processing, 2014, 594, 125-134.	2.6	30
67	On the role of free carboxylic groups and cluster conformation on the surface scratch healing behaviour of ionomers. European Polymer Journal, 2014, 57, 121-126.	2.6	51
68	Effect of strain rate on stress-induced martensitic formation and the compressive properties of Ti–V–(Cr,Fe)–Al alloys. Materials Science & Engineering A: Structural Materials: Properties, Microstructure and Processing, 2013, 573, 111-118.	2.6	32
69	On the use of high precision electrical resistance measurement for analyzing the damage development during accelerated test of Pb-free solder interconnects. , 2013, , .		2
70	Defect-induced Au precipitation in Fe–Au and Fe–Au–B–N alloys studied by in situ small-angle neutron scattering. Acta Materialia, 2013, 61, 7009-7019.	3.8	37
71	Self-healing metallopolymers based on cadmium bis(terpyridine) complex containing polymer networks. Polymer Chemistry, 2013, 4, 4966.	1.9	119
72	Routes to extrinsic and intrinsic self-healing corrosion protective sol-gel coatings: a review. Self-Healing Materials, 2013, 1, 1-18.	1.0	49

#	Article	IF	CITATIONS
73	Switchable static friction of piezoelectric composite—silicon wafer contacts. Applied Physics Letters, 2013, 102, .	1.5	2
74	Modeling and characterization of dielectrophoretically structured piezoelectric composites using piezoceramic particle inclusions with high aspect ratios. Journal of Applied Physics, 2013, 113, 034103.	1.1	4
75	Positron annihilation study of ageing precipitation in deformed Fe–Cu–B–N–C. Philosophical Magazine, 2013, 93, 4182-4197.	0.7	4
76	Multi length scale characterization of austenite in TRIP steels using high-energy X-ray diffraction. Powder Diffraction, 2013, 28, 77-80.	0.4	3
77	High temperature oxidation behaviour of Ti ₂ AlC ceramic at 1200°C. Materials at High Temperatures, 2012, 29, 205-209.	0.5	37
78	Kinetics of phase transformations in steels. , 2012, , 126-156.		1
79	Direct strain energy harvesting in automobile tires using piezoelectric PZT–polymer composites. Smart Materials and Structures, 2012, 21, 015011.	1.8	68
80	Dielectrophoretically structured piezoelectric composites with high aspect ratio piezoelectric particles inclusions. Journal of Applied Physics, 2012, 111, .	1.1	48
81	Influence of Cross-linkers on the Cohesive and Adhesive Self-Healing Ability of Polysulfide-Based Thermosets. ACS Applied Materials & Interfaces, 2012, 4, 6280-6288.	4.0	223
82	High-energy X-ray diffraction study on the temperature-dependent mechanical stability of retained austenite in low-alloyed TRIP steels. Acta Materialia, 2012, 60, 565-577.	3.8	175
83	Numerical study of the scratch-closing behavior of coatings containing an expansive layer. Surface and Coatings Technology, 2012, 206, 2220-2225.	2.2	10
84	Tailoring the release of encapsulated corrosion inhibitors from damaged coatings: Controlled release kinetics by overlapping diffusion fronts. Progress in Organic Coatings, 2012, 75, 20-27.	1.9	28
85	Real-time synchrotron X-ray diffraction study on the isothermal martensite transformation of maraging steel in high magnetic fields. Journal of Applied Crystallography, 2012, 45, 748-757.	1.9	13
86	Tuning the stress induced martensitic formation in titanium alloys by alloy design. Journal of Materials Science, 2012, 47, 4093-4100.	1.7	34
87	Parametric study of multiphase TRIP steels undergoing cyclic loading. Computational Materials Science, 2011, 50, 1490-1498.	1.4	4
88	A critical appraisal of the potential of self healing polymeric coatings. Progress in Organic Coatings, 2011, 72, 211-221.	1.9	227
89	Influence of α morphology and volume fraction on the stress-induced martensitic transformation in Ti–10V–2Fe–3Al. Materials Science & Engineering A: Structural Materials: Properties, Microstructure and Processing, 2011, 528, 5854-5860.	2.6	75
90	In situ synchrotron study on the interplay between martensite formation, texture evolution and load partitioning in low-alloyed TRIP steels. Materials Science & Engineering A: Structural Materials: Properties, Microstructure and Processing, 2011, 528, 6407-6416.	2.6	68

#	Article	IF	CITATIONS
91	Mechanical properties of low temperature synthesized dense and fine-grained Cr2AlC ceramics. Journal of the European Ceramic Society, 2011, 31, 217-224.	2.8	79
92	Ultra-high temperature ablation behavior of Ti2AlC ceramics under an oxyacetylene flame. Journal of the European Ceramic Society, 2011, 31, 855-862.	2.8	64
93	Liquid crystal main-chain polymers for high-performance fibre applications. Liquid Crystals, 2011, 38, 1591-1605.	0.9	51
94	Genetic design and characterization of novel ultra-high-strength stainless steels strengthened by Ni3Ti intermetallic nanoprecipitates. Acta Materialia, 2010, 58, 3582-3593.	3.8	56
95	A new ultrahigh-strength stainless steel strengthened by various coexisting nanoprecipitates. Acta Materialia, 2010, 58, 4067-4075.	3.8	92
96	Development of temperature stable charge based piezoelectric composite quasi-static pressure sensors. Sensors and Actuators A: Physical, 2010, 163, 25-31.	2.0	12
97	Real-time martensitic transformation kinetics in maraging steel under high magnetic fields. Materials Science & Engineering A: Structural Materials: Properties, Microstructure and Processing, 2010, 527, 5241-5245.	2.6	46
98	Liquid crystalline matrix polymers for aramid ballistic composites. Polymer Composites, 2010, 31, 612-619.	2.3	12
99	Properties of Quasi 1-3 Piezoelectric PZT-epoxy Composites Obtained by Dielectrophoresis. Integrated Ferroelectrics, 2010, 114, 108-118.	0.3	8
100	<i>In situ</i> determination of aging precipitation in deformed Fe-Cu and Fe-Cu-B-N alloys by time-resolved small-angle neutron scattering. Physical Review B, 2010, 82, .	1.1	56
101	Thermally activated precipitation at deformation-induced defects in Fe-Cu and Fe-Cu-B-N alloys studied by positron annihilation spectroscopy. Physical Review B, 2010, 81, .	1.1	59
102	Routes and mechanisms towards self healing behaviour in engineering materials. Bulletin of the Polish Academy of Sciences: Technical Sciences, 2010, 58, .	0.8	11
103	Improving the d33 and g33 properties of 0-3 piezoelectric composites by dielectrophoresis. Journal of Applied Physics, 2010, 107, .	1.1	79
104	Bidirectional current-voltage converters based on magnetostrictive/piezoelectric composites. Applied Physics Letters, 2009, 94, 263504.	1.5	17
105	THE COMPOSITION AND TEMPERATURE EFFECTS ON THE ULTRA HIGH STRENGTH STAINLESS STEEL DESIGN. International Journal of Modern Physics B, 2009, 23, 1060-1065.	1.0	1
106	Computational design of UHS maraging stainless steels incorporating composition as well as austenitisation and ageing temperatures as optimisation parameters. Philosophical Magazine, 2009, 89, 1647-1661.	0.7	19
107	Structure and properties of aramid fibres. , 2009, , 394-412.		4
108	On the production and properties of novel particulate NiTip/AA2124 metal matrix composites. Materials Science & Engineering A: Structural Materials: Properties, Microstructure and Processing, 2009, 526, 250-252.	2.6	13

#	Article	IF	CITATIONS
109	A mathematical analysis of physiological and morphological aspects of wound closure. Journal of Mathematical Biology, 2009, 59, 605-630.	0.8	54
110	The effect of aluminium and phosphorus on the stability of individual austenite grains in TRIP steels. Acta Materialia, 2009, 57, 533-543.	3.8	80
111	Modelling strength and ductility of ultrafine grained BCC and FCC alloys using irreversible thermodynamics. Materials Science and Technology, 2009, 25, 833-839.	0.8	97
112	On measurement of retained austenite in multiphase TRIP steels — results of blind round robin test involving six different techniques. Materials Science and Technology, 2009, 25, 567-574.	0.8	75
113	Plasticity induced transformation in a metastable <i>β</i> Ti-1023 alloy by controlled heat treatments. Materials Science and Technology, 2009, 25, 1351-1358.	0.8	58
114	A combined optimization of alloy composition and aging temperature in designing new UHS precipitation hardenable stainless steels. Computational Materials Science, 2009, 45, 467-473.	1.4	29
115	On the transformation behaviour of NiTi particulate reinforced AA2124 composites. Journal of Alloys and Compounds, 2009, 477, 307-315.	2.8	34
116	Computing Interfaces in Diverse Applications. , 2009, , 327-341.		0
117	Self-healing behaviour in man-made engineering materials: bioinspired but taking into account their intrinsic character. Philosophical Transactions Series A, Mathematical, Physical, and Engineering Sciences, 2009, 367, 1689-1704.	1.6	99
118	The Role of Nucleation Behavior in Phase-Field Simulations of the Austenite to Ferrite Transformation. Metallurgical and Materials Transactions A: Physical Metallurgy and Materials Science, 2008, 39, 1237-1247.	1.1	35
119	The isothermal martensite formation in a maraging steel: A magnetic study. Materials Science & Engineering A: Structural Materials: Properties, Microstructure and Processing, 2008, 481-482, 757-761.	2.6	19
120	Isothermal martensitic transformation in a 12Cr–9Ni–4Mo–2Cu stainless steel in applied magnetic fields. Journal of Magnetism and Magnetic Materials, 2008, 320, 1722-1728.	1.0	39
121	Moisture induced crack filling in barrier coatings containing montmorillonite as an expandable phase. Surface and Coatings Technology, 2008, 202, 3346-3353.	2.2	40
122	Oxidation-induced crack healing in Ti3AlC2 ceramics. Scripta Materialia, 2008, 58, 13-16.	2.6	198
123	Early stages of oxidation of Ti3AlC2 ceramics. Materials Chemistry and Physics, 2008, 112, 762-768.	2.0	57
124	Designing nanoprecipitation strengthened UHS stainless steels combining genetic algorithms and thermodynamics. Computational Materials Science, 2008, 44, 678-689.	1.4	51
125	Irreversible thermodynamics modelling of plastic deformation of metals. Materials Science and Technology, 2008, 24, 495-500.	0.8	56
126	Transformation-induced plasticity in multiphase steels subjected to thermomechanical loading. Philosophical Magazine, 2008, 88, 3369-3387.	0.7	16

#	Article	IF	CITATIONS
127	Genetic alloy design based on thermodynamics and kinetics. Philosophical Magazine, 2008, 88, 1825-1833.	0.7	27
128	Modelling steady state deformation of fcc metals by non-equilibrium thermodynamics. Materials Science and Technology, 2007, 23, 1105-1108.	0.8	20
129	Micromechanics-based modelling of properties and failure of multiphase steels. Computational Materials Science, 2007, 39, 17-22.	1.4	54
130	A three-dimensional model for particle dissolution in binary alloys. Computational Materials Science, 2007, 39, 767-774.	1.4	23
131	Micromechanical predictions of TRIP steel behavior as a function of microstructural parameters. Computational Materials Science, 2007, 41, 107-116.	1.4	43
132	Barrier-free heterogeneous grain nucleation in polycrystalline materials: The austenite to ferrite phase transformation in steel. Acta Materialia, 2007, 55, 4489-4498.	3.8	31
133	Characterization of individual retained austenite grains and their stability in low-alloyed TRIP steels. Acta Materialia, 2007, 55, 6713-6723.	3.8	226
134	Laser-ultrasonic monitoring of ferrite recovery in ultra low carbon steel. Materials Science & Engineering A: Structural Materials: Properties, Microstructure and Processing, 2007, 458, 391-401.	2.6	7
135	Modelling and characterization of chi-phase grain boundary precipitation during aging of Fe–Cr–Ni–Mo stainless steel. Materials Science & Engineering A: Structural Materials: Properties, Microstructure and Processing, 2007, 467, 24-32.	2.6	38
136	Positron annihilation spectroscopy as a tool to develop self healing in aluminium alloys. Physica Status Solidi C: Current Topics in Solid State Physics, 2007, 4, 3469-3472.	0.8	13
137	A new etching route for revealing the austenite grain boundaries in an 11.4% Cr precipitation hardening semi-austenitic stainless steel. Materials Characterization, 2007, 58, 455-460.	1.9	36
138	Martensitic transformation of individual grains in low-alloyed TRIP steels. Scripta Materialia, 2007, 56, 421-424.	2.6	245
139	Laser beam welding of an Oxide Dispersion Strengthened super alloy. Journal of Materials Science, 2007, 42, 5286-5295.	1.7	21
140	A comparison of numerical models for one-dimensional Stefan problems. Journal of Computational and Applied Mathematics, 2006, 192, 445-459.	1.1	126
141	Analysis of γ→α transformation in a Nb micro-alloyed C–Mn steel by phase field modelling. Acta Materialia, 2006, 54, 1431-1440.	3.8	81
142	Phase transformations in steel studied by 3DXRD microscopy. Nuclear Instruments & Methods in Physics Research B, 2006, 246, 194-200.	0.6	32
143	Modification of a Thermomechanical Model to Predict Constitutive Behavior of Al-Mg-Si Alloys. Journal of Materials Engineering and Performance, 2006, 15, 632-639.	1.2	5
144	Modeling recrystallization kinetics in AA1050 following simulated breakdown rolling. Metallurgical and Materials Transactions A: Physical Metallurgy and Materials Science, 2006, 37, 2859-2869.	1.1	7

#	Article	IF	CITATIONS
145	Modelling of the effects of grain orientation on transformation-induced plasticity in multiphase carbon steels. Modelling and Simulation in Materials Science and Engineering, 2006, 14, 617-636.	0.8	59
146	Experimental observations elucidating the mechanisms of structural bcc-hcp transformations inl²â^'Tialloys. Physical Review B, 2006, 74, .	1.1	24
147	Ferrite/Pearlite Band Prevention in Dual Phase and TRIP Steels: Model Development. ISIJ International, 2005, 45, 380-387.	0.6	27
148	Advanced Models for Particle Dissolution in Multi-Component Alloys. , 2005, , 53-60.		0
149	The dependence of the β-AlFeSi to α-Al(FeMn)Si transformation kinetics in Al–Mg–Si alloys on the alloying elements. Materials Science & Engineering A: Structural Materials: Properties, Microstructure and Processing, 2005, 394, 9-19.	2.6	151
150	3DXRD microscopy for the study of solid-state phase transformation kinetics. Nuclear Instruments & Methods in Physics Research B, 2005, 238, 107-110.	0.6	4
151	Theory for diffusional transformation kinetics: Multicomponent and multiphase systems. Scripta Materialia, 2005, 53, 1089-1094.	2.6	3
152	Cross-diffusion controlled particle dissolution in metallic alloys. Computing and Visualization in Science, 2005, 8, 27-33.	1.2	5
153	Analysis of the γ → α transformation in a C-Mn steel by phase-field modeling. Metallurgical and Materials Transactions A: Physical Metallurgy and Materials Science, 2005, 36, 2327-2340.	1.1	53
154	Investigation of Ferrite Softening Processes in a 0.2 wt% C 1.5 wt% Mn Steel after Hot Deformation. , 2005, , 175-180.		0
155	The Effect of Grain Geometry on the Kinetics of Recrystallisation Processes. , 2005, , 96-101.		Ο
156	Phase field modelling of the interfacial condition at the moving interphase during the γ→α transformation in C–Mn steels. Computational Materials Science, 2005, 34, 290-297.	1.4	22
157	A morphological study of filiform corrosive attack on cerated AA2024-T351 aluminium alloy. Corrosion Science, 2005, 47, 107-124.	3.0	25
158	An integrated study on the effect of pre- and post-extrusion heat treatments and surface treatment on the filiform corrosion properties of an aluminium extrusion alloy. Corrosion Science, 2005, 47, 2711-2730.	3.0	25
159	High-temperature magnetisation measurements on the pearlite transformation kinetics in nearly eutectoid steel. Journal of Magnetism and Magnetic Materials, 2004, 268, 40-48.	1.0	5
160	Property Optimisation in Fibre Metal Laminates. Applied Composite Materials, 2004, 11, 63-76.	1.3	18
161	A single-grain approach applied to the modeling of recrystallization kinetics for cold-rolled single-phase metals. Metallurgical and Materials Transactions A: Physical Metallurgy and Materials Science, 2004, 35, 741-749.	1.1	17
162	A model for ferrite/pearlite band formation and prevention in steels. Metallurgical and Materials Transactions A: Physical Metallurgy and Materials Science, 2004, 35, 425-433.	1.1	29

#	Article	IF	CITATIONS
163	Neutron depolarisation study of the austenite grain size in TRIP steels. Physica B: Condensed Matter, 2004, 350, E463-E466.	1.3	6
164	Solid-state phase transformations involving solute partitioning: modeling and measuring on the level of individual grains. Acta Materialia, 2004, 52, 4757-4766.	3.8	46
165	A morphological study of filiform corrosive attack on chromated and alkaline-cleaned AA2024-T351 aluminium alloy. Corrosion Science, 2004, 46, 1201-1224.	3.0	26
166	Assuring Microstructural Homegeniety in Dual Phase and Trip Steels. Steel Research International, 2004, 75, 711-715.	1.0	6
167	A Study on the β′ and β Formation Kinetics in AA6063 Using Differential Scanning Calorimetry. Journal of Materials Engineering and Performance, 2003, 12, 408-413.	1.2	4
168	Cluster formation of pearlite colonies during the austenite/pearlite phase transformation in eutectoid steel. Physica B: Condensed Matter, 2003, 335, 99-103.	1.3	4
169	Particle dissolution and cross-diffusion in multi-component alloys. Materials Science & Engineering A: Structural Materials: Properties, Microstructure and Processing, 2003, 347, 265-279.	2.6	17
170	In-situ study of pearlite nucleation and growth during isothermal austenite decomposition in nearly eutectoid steel. Acta Materialia, 2003, 51, 3927-3938.	3.8	58
171	In situ observations on the mechanical stability ofÂaustenite in TRIP-steel. European Physical Journal Special Topics, 2003, 104, 499-502.	0.2	15
172	Grain Nucleation and Growth During Phase Transformations. Science, 2002, 298, 1003-1005.	6.0	339
173	Assessment of different techniques for quantification of α-Al(FeMn)Si and β-AlFeSi intermetallics in AA 6xxx alloys. Materials Characterization, 2002, 49, 409-420.	1.9	128
174	Filiform corrosion imaged beneath protection layers on Al alloys. Nuclear Instruments & Methods in Physics Research B, 2002, 190, 365-369.	0.6	10
175	Quantification of the evolution of the 3D intermetallic structure in a 6005A aluminium alloy during a homogenisation treatment. Materials Characterization, 2002, 48, 379-392.	1.9	65
176	High temperature SANS experiments on Nb(C,N) and MnS precipitates in HSLA steel. Metallurgical and Materials Transactions A: Physical Metallurgy and Materials Science, 2002, 33, 1883-1891.	1.1	19
177	Modeling the kinetics of grain-boundary-nucleated recrystallization processes after cold deformation. Metallurgical and Materials Transactions A: Physical Metallurgy and Materials Science, 2002, 33, 529-537.	1.1	16
178	Texture and microstructure development during intercritical rolling of low-carbon steels. Metallurgical and Materials Transactions A: Physical Metallurgy and Materials Science, 2002, 33, 1589-1603.	1.1	19
179	Neutron depolarization study of the austenite/pearlite phase transformation in steel. Applied Physics A: Materials Science and Processing, 2002, 74, s1052-s1054.	1.1	9
180	The influence of nitrogen on the austenite/ferrite interface mobility in Fe–1at.%Si. Materials Science & Engineering A: Structural Materials: Properties, Microstructure and Processing, 2002, 323, 403-408.	2.6	6

#	Article	IF	CITATIONS
181	A mathematical model for the dissolution of stoichiometric particles in multi-component alloys. Materials Science & Engineering A: Structural Materials: Properties, Microstructure and Processing, 2002, 328, 14-25.	2.6	21
182	Ferrite/pearlite band formation in hot rolled medium carbon steel. Materials Science and Technology, 2002, 18, 297-303.	0.8	74
183	Title is missing!. Journal of Materials Science, 2002, 37, 789-794.	1.7	113
184	The effect of mechanical surface patterning on filiform growth characteristics. Journal of Materials Science, 2002, 37, 2755-2761.	1.7	9
185	The effect of β, β′ and β″ precipitates in a homogenised AA6063 alloy on the hot deformability and the peak hardness. Materials Science & Engineering A: Structural Materials: Properties, Microstructure and Processing, 2001, 299, 105-115.	? 2.6	22
186	Effects of nitriding on fatigue strength of quenched and tempered steel: role of interstitial nitrogen. Materials Science and Technology, 2001, 17, 54-62.	0.8	7
187	The application of laser scanning confocal microscopy to tribological research. Wear, 2001, 251, 1159-1168.	1.5	21
188	Magnetic and X-ray diffraction measurements for the determination of retained austenite in TRIP steels. Materials Science & Engineering A: Structural Materials: Properties, Microstructure and Processing, 2001, 313, 145-152.	2.6	206
189	Title is missing!. Journal of Materials Science, 2001, 36, 1863-1871.	1.7	2
190	A study on the fracture toughness of Al-based MMCs containing different volume fractions Al2O3. Journal of Materials Science Letters, 2001, 20, 1147-1150.	0.5	3
191	Dilatometric analysis of phase transformations in hypo-eutectoid steels. Journal of Materials Science, 2001, 36, 519-526.	1.7	150
192	Anisotropic dilatation behaviour during transformation of hot rolled steels showing banded structure. Materials Science and Technology, 2001, 17, 1569-1574.	0.8	57
193	Domain size determination of granular ferromagnetic systems with neutron depolarization. Journal of Applied Physics, 2001, 89, 1275-1280.	1.1	8
194	Modelling the Austenite to Ferrite Phase Transformation in Low Carbon Steels in Terms of the Interface Mobility ISIJ International, 2000, 40, 713-718.	0.6	46
195	A study on the austenite-to-ferrite phase transformation in binary substitutional iron alloys. Materials Science & Engineering A: Structural Materials: Properties, Microstructure and Processing, 2000, 283, 234-241.	2.6	75
196	A three-dimensional model for the development of the microstructure in steel during slow cooling. Materials Science & Engineering A: Structural Materials: Properties, Microstructure and Processing, 2000, 277, 218-228.	2.6	19
197	Field-dependent neutron depolarization study of the ferrite formation in medium-carbon steels. Acta Materialia, 2000, 48, 1105-1114.	3.8	10
198	A filiform corrosion and potentiodynamic polarisation study of some aluminium alloys. Journal of Materials Science, 2000, 35, 1629-1639.	1.7	42

#	Article	IF	CITATIONS
199	On the mobility of the austenite-ferrite interface in Fe-Co and Fe-Cu. Metallurgical and Materials Transactions A: Physical Metallurgy and Materials Science, 2000, 31, 379-385.	1.1	31
200	Comparison of experimental AA6063 extrusion trials to 3D numerical simulations, using a general solute-dependent constitutive model. Computational Materials Science, 2000, 18, 381-392.	1.4	26
201	Phase transformations in low-carbon steels ; modelling the kinetics in terms of the interface mobility. European Physical Journal Special Topics, 1999, 09, Pr9-401-Pr9-409.	0.2	11
202	Neutron depolarization study of phase transformations in steel. Physica B: Condensed Matter, 1999, 267-268, 88-91.	1.3	9
203	Assessment of constitutive equations in modelling the hot deformability of some overaged Al–Mg–Si alloys with varying solute contents. Materials Science & Engineering A: Structural Materials: Properties, Microstructure and Processing, 1999, 266, 135-145.	2.6	37
204	Bainite transformation of low carbon Mn–Si TRIP-assisted multiphase steels: influence of silicon content on cementite precipitation and austenite retention. Materials Science & Engineering A: Structural Materials: Properties, Microstructure and Processing, 1999, 273-275, 475-479.	2.6	119
205	Dissolution of β particles in an Alî—,Mgî—,Si alloy during DSC runs. Materials Science & Engineering A: Structural Materials: Properties, Microstructure and Processing, 1999, 272, 250-256.	2.6	36
206	Modelling fracture in an Al2O3 particle reinforced AA 6061 alloy using Weibull statistics. Journal of Materials Science, 1999, 34, 4097-4104.	1.7	9
207	A microstructural model for predicting hardness profiles of Fe-Cr alloys after nitriding. Philosophical Magazine A: Physics of Condensed Matter, Structure, Defects and Mechanical Properties, 1999, 79, 1193-1206.	0.8	5
208	The Effect of Metalworking Fluids on the Gas-nitriding Behavior of 31CrMoV9 Steel. Journal of Materials Science Letters, 1998, 17, 1215-1217.	0.5	1
209	Precipitation kinetics in Al6061 and in an Al6061-alumina particle composite. Journal of Materials Science, 1998, 33, 4477-4483.	1.7	34
210	The ferrite and austenite lattice parameters of Fe–Co and Fe–Cu binary alloys as a function of temperature. Acta Materialia, 1998, 46, 5223-5228.	3.8	27
211	Simulations of pro-eutectoid ferrite formation using a mixed control growth model. Materials Science & Engineering A: Structural Materials: Properties, Microstructure and Processing, 1998, 246, 104-116.	2.6	25
212	Kinetics of γ → α phase transformation in Fe-Mn alloys containing low manganese. Materials Science and Technology, 1998, 14, 10-18.	0.8	114
213	Analytical approach to particle dissolution in a finite medium. Materials Science and Technology, 1997, 13, 308-312.	0.8	13
214	The influence of the nitriding temperature on the fatigue limit of 42CrMo4 and En40B steel. Journal of Materials Science Letters, 1997, 16, 1327-1329.	0.5	3
215	Neutron depolarization as a tool for studying phase transformations in steels. Physica B: Condensed Matter, 1997, 234-236, 1027-1029.	1.3	6
216	The apparent activation energy for the dissolution of spherical Si-particles in AlSi-alloys. Materials Science & Engineering A: Structural Materials: Properties, Microstructure and Processing, 1997, 231, 80-89.	2.6	6

#	Article	IF	CITATIONS
217	Prediction of jominy hardness profiles of steels using artificial neural networks. Journal of Materials Engineering and Performance, 1996, 5, 57-63.	1.2	35
218	A numerical model for the dissolution of spherical particles in binary alloys under mixed mode control. Materials Science & Engineering A: Structural Materials: Properties, Microstructure and Processing, 1996, 220, 140-146.	2.6	28
219	Analysis of phase transformation in Fe-C alloys using differential scanning calorimetry. Journal of Materials Science, 1996, 31, 1501-1508.	1.7	33
220	An in situ hot stage transmission electron microscopy study of the decomposition of Fe-C austenites. Journal of Materials Science, 1995, 30, 6223-6234.	1.7	50
221	The effect of local distortions in the intermolecular hydrogen bond network on the lifetime of aramid yarns. Journal of Materials Science Letters, 1995, 14, 1440-1443.	0.5	2
222	The kinetics of the internal nitriding of Fe-2 at. pct Al alloy. Metallurgical and Materials Transactions A: Physical Metallurgy and Materials Science, 1995, 26, 765-776.	1.1	72
223	Analysis of the nitrogen absorption isotherms of cold-rolled Fe-2 at.% Al specimens with different AIN precipitate dimensions. Philosophical Magazine A: Physics of Condensed Matter, Structure, Defects and Mechanical Properties, 1995, 72, 931-947.	0.8	36
224	The lattice parameters of austenite and ferrite in Feî—,C alloys as functions of carbon concentration and temperature. Scripta Metallurgica Et Materialia, 1993, 29, 1011-1016.	1.0	212
225	Molecular and macroscopic orientational order in aramid solutions: a model to explain the influence of some spinning parameters on the modulus of aramid yarns. Polymer, 1992, 33, 2998-3006.	1.8	40
226	The Concept of Filament Strength and the Weibull Modulus. Journal of Testing and Evaluation, 1989, 17, 292-298.	0.4	133
227	The effect of double layer coatings of high modulus on contact stresses. Philosophical Magazine A: Physics of Condensed Matter, Structure, Defects and Mechanical Properties, 1986, 53, 101-111.	0.8	22
228	Change of viscosity during structural relaxation of amorphous Fe40Ni40B20. Acta Metallurgica, 1986, 34, 483-492.	2.1	64
229	A semi-quantitative description of the kinetics of structural relaxation in amorphous Fe40Ni40B20. Acta Metallurgica, 1984, 32, 1895-1902.	2.1	93
230	Plastic processes in a range of soda-lime-silica glasses. Journal of Non-Crystalline Solids, 1984, 64, 249-268.	1.5	42
231	Accurate contraction and creep measurements during structural relaxation of amorphous Fe40Ni40B20. Scripta Metallurgica, 1984, 18, 515-519.	1.2	30
232	Rain erosion damage in brittle materials. Engineering Fracture Mechanics, 1983, 17, 367-379.	2.0	26
233	Indentation and liquid impact studies on coated germanium. Philosophical Magazine A: Physics of Condensed Matter, Structure, Defects and Mechanical Properties, 1983, 48, 767-777.	0.8	13
234	The effect of thin hard coatings on the Hertzian stress field. Philosophical Magazine A: Physics of Condensed Matter, Structure, Defects and Mechanical Properties, 1982, 46, 133-150.	0.8	82

#	Article	IF	CITATIONS
235	Liquid jet impact damage on zinc sulphide. Journal of Materials Science, 1982, 17, 2625-2636.	1.7	19
236	Studies of contact damage in polycrystalline zinc sulphide. Journal of Materials Science, 1980, 15, 2965-2972.	1.7	43
237	Toughening of a ZrC Particle-Reinforced Ti3AIC2 Composite. Ceramic Engineering and Science Proceedings, 0, , 31-39.	0.1	4